# Comparing phenomenological recipes with a microscopic model for the electric amplitude in strangeness photoproduction

A. Yu. Korchin[1,2,*] and O. Scholten[1,†]
[1]*Kernfysisch Versneller Instituut, University of Groningen, 9747 AA Groningen, The Netherlands*
[2]*NSC "Kharkov Institute of Physics and Technology," 61108 Kharkov, Ukraine*
(Received 13 June 2003; published 15 October 2003)

Corrections to the Born approximation in photoinduced strangeness production off a proton are calculated in a semirealistic microscopic model. The vertex corrections and internal contributions to the amplitude of the $\gamma p \to K^+\Lambda$ reaction are included on the one-loop level. Different gauge-invariant phenomenological prescriptions for the modification of the Born contribution via the introduction of form factors and contact terms are discussed. In particular, it is shown that the popular minimal-substitution method of Ohta corresponds to a special limit of the more realistic approach.

DOI: 10.1103/PhysRevC.68.045206 PACS number(s): 13.40.−f, 13.60.Le, 13.75.Jz

## I. INTRODUCTION

One of the goals in studies of photoproduction and electroproduction of pions or kaons on the proton is the extraction of information on baryon resonances [1]. This is usually done on the basis of models built on effective Lagrangians [2–5]. A typical amplitude, describing meson photoproduction, includes the Born contribution as a kind of background to be added to the resonance contributions. Only at low photon energies the physics is determined by the Born diagrams. With increasing photon energy the Born contribution rises to produce unrealistically large cross sections at energies of interest for strangeness production as noticed by many authors [6–8]. The popular strategy is to suppress the Born amplitude by including form factors (FF's) in the strong-interaction vertices. These FF's account for physics on the scales beyond what is considered, i.e., exchanges of heavier mesons which are truncated from the Lagrangian and (higher order) loop corrections which are omitted for simplicity. Closely associated with FF's are additional terms, called contact terms (sometimes four-point vertices or internal contributions), which restore gauge invariance (GI) usually violated by the introduction of FF's. Several different prescriptions for the FF's and contact terms are commonly in use. While at low energies these prescriptions lead to relatively close results, at higher energies the calculated cross sections may differ drastically. Therefore the information on the properties of resonances extracted from these processes is strongly influenced by uncertainties in the treatment of this problem [4].

In the present work we study two commonly used procedures: Ohta's minimal-substitution method [9] and the Davidson-Workman (DW) recipe [8,10]. The most essential difference in predictions of these two methods for the meson photoproduction processes, such as $\gamma N \to \pi N$ or $\gamma p \to K^+\Lambda(K\Sigma)$, is the modification of one particular invariant amplitude $A_2(s,t)$. This amplitude is related to the electric part of the amplitude and originates from the convection current of the charged particles involved in the reaction. Its contribution to the matrix element, being proportional to the momenta of particles, affects the cross section at high energies. In the approach of Ohta $A_2(s,t)$ is not altered, due to the complete cancellation between the effects of FF's and the contact terms. In other methods, in particular in the DW approach [8,10], or Haberzettl's approach [11,7], the amplitude $A_2(s,t)$ changes considerably compared to the Born amplitude.

In order to study different phenomenological approaches we calculate vertex corrections and internal contributions to the electric amplitude in an effective Lagrangian model. Irreducible one-loop contributions are included for the reaction $\gamma p \to K^+\Lambda$. This allows us to extract, within a gauge-invariant model, both the FF's (associated with three-point loop corrections) and the contact terms (associated with four-point loop corrections), and to make a comparison with phenomenological approaches. The model is $SU(3)_{flavor}$ symmetrical and describes the baryon-meson interaction as well as the meson-meson interaction of the scalar and pseudoscalar mesons. In the intermediate states of the diagrams we include the scalar meson, kaon, proton, and $\Lambda$ hyperon. The pion and $\Sigma$ hyperon are not included as yet, and thus the model can be considered as semirealistic. On the one-loop level there appear three diagrams for the $K^+p\Lambda$ vertex and four diagrams for the internal amplitude. The vertex corrections have the property that in the limit of large mass of the scalar meson each of the three vertex-correction diagrams generates FF's, which depend exclusively on one of the Mandelstam variables $s,u$, or $t$. This in turn leads to an interesting effect of cancellation between the vertex corrections and the four-point diagrams in the scalar amplitude $A_2(s,t)$.

We should mention that some loop contributions in the pion photoproduction on the nucleon were studied in Ref. [12], where the need for consistent treatment of corrections to the Born amplitude was stressed.

The paper is organized as follows. In Sec. II A the Born approximation is briefly discussed and invariant amplitudes are introduced. The structure of $K^+p\Lambda$ vertex is addressed in Sec. II B. Different recipes for restoring GI are outlined. The

*Electronic address: korchin@kvi.nl
†Electronic address: scholten@kvi.nl; http://www.kvi.nl/scholten

 

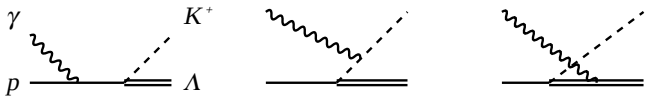


FIG. 1. Born diagrams for the reaction $\gamma+p\to K^+ +\Lambda$. Solid lines depict the proton, double-solid lines—the $\Lambda$ hyperon, wavy lines—the photon, and dashed lines—the kaon.

present model for calculation of the loop corrections and the parameters is described in Sec. II C. Results of calculations and a discussion are presented in Sec. III. In Sec. IV we draw conclusions. Finally, the Appendix contains details of the calculation of the three- and four-point loop integrals.

## II. FORMALISM

### A. Born diagrams

The Born amplitude for the reaction $\gamma+p\to K^+ +\Lambda$ (see Fig. 1) can be split in electric and magnetic parts, i.e., $\mathcal{T}^\mu_B=\mathcal{T}^\mu_{B,El}+\mathcal{T}^\mu_{B,Mag}$, where

$$\mathcal{T}^\mu_{B,El}=eg\bar{u}(p')\gamma_5 u(p)\left(\frac{2p^\mu}{s-M_N^2}+\frac{2q^\mu}{t-\mu_k^2}\right),$$

$$\mathcal{T}^\mu_{B,Mag}=eg\bar{u}(p')\gamma_5 \times\left\{\frac{1}{s-M_N^2}\left[(1+\kappa_p)\gamma^\mu \not{k}+\frac{\kappa_p}{M_N}(\gamma^\mu k\cdot p-p^\mu \not{k})\right]+\frac{1}{u-M_\Lambda^2}\left[-\kappa_\Lambda\gamma^\mu\not{k}+\frac{\kappa_\Lambda}{M_\Lambda}(\gamma^\mu k\cdot p'-p'^\mu\not{k})\right]\right\}u(p). \tag{1}$$

The four-momenta of the (real) photon, proton, kaon, and $\Lambda$ are denoted by $k,p,q$, and $p'$ respectively, and $M_N,\mu_k$, and $M_\Lambda$ are the masses of the proton, kaon, and $\Lambda$. The invariants $s,t,u$ are the Mandelstam variables satisfying the relation $s+t+u=M_N^2+M_\Lambda^2+\mu_k^2$. The anomalous magnetic moments of the proton and $\Lambda$ are denoted by $\kappa_p$ and $\kappa_\Lambda$, respectively. Finally, $g$ stands for the $K^+p\Lambda$ coupling constant. The spinor of the initial proton is $u(p)$, and the one of the final $\Lambda$ is $\bar{u}(p')$ where the helicity (spin) indices are suppressed. The amplitudes in Eqs. (1) are gauge invariant, i.e., $k\cdot\mathcal{T}_{El}=k\cdot\mathcal{T}_{Mag}=0$.

We will use the formalism [13,14] in which the amplitude is decomposed through the independent spin tensors

$$\mathcal{T}^\mu=\sum_{i=1}^{4}A_i(s,t)\bar{u}(p')\mathcal{M}_i^\mu u(p), \tag{2}$$

with

$$\mathcal{M}_1^\mu=-\gamma_5\gamma^\mu\not{k},$$

$$\mathcal{M}_2^\mu=2\gamma_5(p^\mu k\cdot p'-p'^\mu k\cdot p),$$

$$\mathcal{M}_3^\mu=\gamma_5(\gamma^\mu k\cdot p-p^\mu\not{k}),$$

$$\mathcal{M}_4^\mu=\gamma_5(\gamma^\mu k\cdot p'-p'^\mu\not{k}). \tag{3}$$

The gauge-invariant basis $\mathcal{M}_i^\mu$ is constructed in such a way that the scalar amplitudes $A_i(s,t)$ are free from kinematical singularities and zeros [14]. For the Born diagrams $A_i$ take the form (we omit arguments for brevity)

$$A_1^{Born}=eg\left(\frac{1+\kappa_p}{s-M_N^2}+\frac{\kappa_\Lambda}{u-M_\Lambda^2}\right),$$

$$A_2^{Born}=eg\frac{2}{(s-M_N^2)(t-\mu_K^2)},$$

$$A_3^{Born}=eg\frac{\kappa_p}{M_N}\frac{1}{s-M_N^2}, \tag{4}$$

$$A_4^{Born}=eg\frac{\kappa_\Lambda}{M_\Lambda}\frac{1}{u-M_\Lambda^2}.$$

The magnetic part results in the single-pole amplitudes $A_1^{Born},A_3^{Born}$, and $A_4^{Born}$, while the electric part contributes solely to the double-pole amplitude $A_2^{Born}$. As was discussed in Ref. [14] the latter is a peculiar feature of the amplitude with real photons and the choice of the spin tensors $\mathcal{M}_i^\mu$.

### B. $K^+p\Lambda$ vertex and form factors

In a phenomenological description strong FF's are often included directly in the Born diagrams. At this point we recall the general structure of the $K^+p\Lambda$ vertex

$$\Gamma(p',p;q)=g\left(\gamma_5 f_1+\gamma_5\frac{\not{p}-M_N}{M_N}f_2+\frac{\not{p}'-M_\Lambda}{M_\Lambda}\gamma_5 f_3+\frac{\not{p}'-M_\Lambda}{M_\Lambda}\gamma_5\frac{\not{p}-M_N}{M_N}f_4\right), \tag{5}$$

where $p',p$, and $q$ are the $\Lambda$, proton, and kaon momenta, respectively, and $f_i\equiv f_i(p'^2,p^2,q^2)$ are scalar functions. If only one of the hadrons is off its mass shell then Eq. (5) simplifies. For this situation it is convenient to introduce the three-point FF's:

$$F_s(p^2)=f_1(M_\Lambda^2,p^2,\mu_K^2),$$

$$F_u(p'^2)=f_1(p'^2,M_N^2,\mu_K^2),$$

$$F_t(q^2)=f_1(M_\Lambda^2,M_N^2,q^2), \tag{6}$$

$$G_s(p^2)=f_2(M_\Lambda^2,p^2,\mu_K^2),$$

$$G_u(p'^2)=f_3(p'^2,M_N^2,\mu_K^2).$$

In general the functions $F_s(p^2),F_u(p'^2)$, and $F_t(q^2)$ have different functional dependencies as indicated by the subscript $s,u$, or $t$, and are normalized to unity on the mass shell.

When the vertex in Eq. (5) is included in the tree-level terms, the magnetic amplitude $\mathcal{T}^{\mu}_{B,Mag}$ in Eq. (1) is modified to $\mathcal{T}^{\mu}_{Mag}$ with the following result for the scalar amplitudes:

$$A_{1,Mag} = eg\left(\frac{1+\kappa_p}{s-M_N^2}F_s(s) + \frac{\kappa_\Lambda}{u-M_\Lambda^2}F_u(u) + G_s(s)\frac{\kappa_p}{2M_N^2} + G_u(u)\frac{\kappa_\Lambda}{2M_\Lambda^2}\right),$$

$$A_{3,Mag} = eg\left(\frac{\kappa_p}{M_N}\frac{1}{s-M_N^2}F_s(s) + \frac{2}{M_N}\frac{1}{s-M_N^2}G_s(s)\right),$$

$$A_{4,Mag} = eg\frac{\kappa_\Lambda}{M_\Lambda}\frac{1}{u-M_\Lambda^2}F_u(u). \tag{7}$$

The electric amplitude changes to

$$\mathcal{T}^{\mu}_{El} = eg\bar{u}(p')\gamma_5\left(\frac{2p^\mu}{s-M_N^2}\left[F_s(s) + G_s(s)\frac{\not{k}}{M_N}\right] + \frac{2q^\mu}{t-\mu_k^2}F_t(t)\right)u(p). \tag{8}$$

This term cannot be cast in the form of Eq. (2) since it is not gauge invariant. Indeed, contraction with the photon momentum results in

$$k\cdot\mathcal{T}_{El} = eg\bar{u}(p')\gamma_5\left[F_s(s) + G_s(s)\frac{\not{k}}{M_N} - F_t(t)\right]u(p) = e\bar{u}(p')[\Gamma(p', p+k; q) - \Gamma(p', p; q-k)]u(p) \neq 0. \tag{9}$$

In general, it is known that there are other contributions to the amplitude [15,16,12] which ensure GI of the total amplitude. We will denote this additional amplitude by $\mathcal{T}^{\mu}_c$ and discuss different ways of constructing this amplitude.

#### *1. Minimal-substitution method of Ohta [9]*

In the original formulation of Ohta [9] the electromagnetic interaction (EM) was included directly in the three-point $\pi NN$ vertex using the minimal-substitution method. This allowed for construction of $\mathcal{T}^{\mu}_c$ in terms of the FF's. It may be instructive to derive the same result (for the $pK^+\Lambda$ vertex) using a simpler, though less rigorous, method which was applied in Ref. [17]. The GI requirement for the total amplitude $T_{Mag}+\mathcal{T}_{El}+\mathcal{T}_c$, with the help of Eq. (9) and definitions $s-M_N^2=2k\cdot p$, $t-\mu_k^2=-2k\cdot q$, can be written as

$$k\cdot\mathcal{T}_c = -k\cdot\mathcal{T}_{El} = egk_\mu\bar{u}(p')\gamma_5\left(2p^\mu\frac{1-F_s(s)}{s-M_N^2} + 2q^\mu\frac{1-F_t(t)}{t-\mu_K^2} - G_s(s)\frac{\gamma^\mu}{M_N}\right)u(p), \tag{10}$$

from which $\mathcal{T}^{\mu}_c$ is obtained as the term multiplying $k_\mu$. We now find [using Eq. (8)]

$$\mathcal{T}^{\mu}_{El} + \mathcal{T}^{\mu}_c = eg\bar{u}(p')\gamma_5\left[\frac{2p^\mu}{s-M_N^2} + \frac{2q^\mu}{t-\mu_K^2} + G_s(s)\frac{1}{M_N}\left(\frac{p^\mu}{k\cdot p}\not{k} - \gamma^\mu\right)\right]u(p) \tag{11}$$

up to the transverse terms which are not constrained by the condition of GI. The amplitude in Eq. (11) is apparently gauge invariant and yields two scalar amplitudes

$$A_{2,El} = eg\frac{2}{(s-M_N^2)(t-\mu_K^2)},$$

$$A_{3,El} = -eg\frac{1}{M_N}\frac{2}{s-M_N^2}G_s(s). \tag{12}$$

It is seen that, first, $A_{3,El}$ cancels the term in $A_{3,Mag}$ proportional to $G_s(s)$, and second, the amplitude $A_{2,El}$ coincides with the Born amplitude $A_2^{Born}$ in Eq. (4). The main result is thus that the scalar amplitude $A_2$ is not modified in the presence of strong FF's, as noticed earlier in Ref. [6].

#### *2. Approach of Davidson and Workman [8]*

In order to change the electric contribution in a phenomenological approach some authors introduced FF's directly in the amplitude $A_2$ in Eq. (2). As was pointed out in Refs. [8,10], care should be taken with the structure of these FF's in order to avoid spurious pole contributions as generated with the original introduction of these FF's in Refs. [11,7]. The procedure in Refs. [8,10], in which the FF's modify the total amplitude $A_2$, will be referred to as the DW approach.

In the DW approach the amplitude $A_2$ is modified to

$$A_2 = A_2^{Born}\hat{F} = A_2^{Born} + eg\frac{2}{(s-M_N^2)(t-\mu_K^2)}(\hat{F}-1) \equiv A_2^{Born} + \Delta A_2^{DW}, \tag{13}$$

where the factor $\hat{F}$ for the reaction $\gamma p\to K^+\Lambda$ is chosen to be

$$\hat{F} = F_s(s) + F_t(t) - F_s(s)F_t(t), \tag{14}$$

to ensure that the correction to the Born contribution is free from poles at $s=M_N^2$ and $t=\mu_K^2$. The functions $F_s(s)$ and $F_t(t)$ are normalized to unity on shell and are usually parametrized in the monopole or dipole form but are not necessarily related to the FF's introduced in Sec. II B.

### C. Loop contributions

In a microscopic model for the reaction mechanism there are various loop corrections to the Born diagrams. The simplest loop corrections are self-energy insertions in the propagators. These corrections are partially compensated by the three-point loop corrections to the EM vertices $\gamma pp$ and $\gamma KK$. The net result is that only the magnetic contribution is affected, however the convection current, which is of our main concern, remains unchanged. For this reason these loop

contributions will not be included. We will come back to this issue in the end of Sec. III B. The second type of loop diagrams are corrections to the $K^+p\Lambda$ vertex shown in Fig. 2(a). These are ordered in a particular way to allow for an interpretation in terms of the three-point FF's introduced in Sec. II B. In this section we will explicitly calculate the three-point loop corrections, $\mathcal{L}^\mu_{[3]}$, to the electric amplitude. As discussed in Sec. II B, GI of the full amplitude is restored after inclusion of the four-point diagrams (internal amplitude) depicted in Fig. 2(b). These diagrams can be obtained by attaching the photon to the lines of charged intermediate particles in the three-point loops and will be referred to as $\mathcal{L}^\mu_{[4]}$.

The amplitude $\mathcal{L}^\mu_{[4]}$ cannot be expanded in the basis, Eq. (2), since only the sum $\mathcal{L}^\mu_{[3]}+\mathcal{L}^\mu_{[4]}$ is gauge invariant. To extract the amplitude $A_2$ we express the loop corrections in terms of the Lorentz structures appearing in Eq. (2): $\gamma_5 p^\mu, \gamma_5 q^\mu, \gamma_5\gamma^\mu, \gamma_5 p^\mu \not{k}, \gamma_5 q^\mu \not{k}, \gamma_5\gamma^\mu \not{k}$, where it can be noted that $\mathcal{M}^\mu_2 = 2\gamma_5(q^\mu k\cdot p - p^\mu k\cdot q)$ and $\mathcal{M}^\mu_4 = \mathcal{M}^\mu_3 + \gamma_5(q^\mu \not{k} - \gamma^\mu k\cdot q)$. Since $\mathcal{M}^\mu_2$ is expressed solely in terms of $\gamma_5 p^\mu$ and $\gamma_5 q^\mu$, it will be sufficient to retain only these terms from the loop corrections and write

$$\mathcal{L}^\mu_{[3]} = 2eg\bar{u}(p')\gamma_5\left(p^\mu\frac{F_s(s)-1}{s-M_N^2} + q^\mu\frac{F_t(t)-1}{t-\mu_k^2}\right)u(p) + \cdots, \tag{15}$$

$$\mathcal{L}^\mu_{[4]} = 2eg\bar{u}(p')\gamma_5[p^\mu H_s(s,t) + q^\mu H_t(s,t)]u(p) + \cdots, \tag{16}$$

where the ellipses mean the omitted terms containing the Lorentz tensors $\mathcal{M}^\mu_1, \mathcal{M}^\mu_3$, and $\mathcal{M}^\mu_4$ appearing in the magnetic terms. It should be noted that the functions $F_t(t)$ and $F_s(s)$ in the loop correction $\mathcal{L}^\mu_{[3]}$, Eq. (15), coincide with the phenomenological FF's appearing in Eq. (8). The condition of GI, $k\cdot(\mathcal{L}_{[3]}+\mathcal{L}_{[4]})=0$, imposes the relation

$$(s-M_N^2)H_s(s,t) - (t-\mu_K^2)H_t(s,t) = F_t(t) - F_s(s). \tag{17}$$

The correction to the Born amplitude $A_2^{Born}$ can now be expressed as

$$\begin{aligned}\Delta A_2 &= eg\frac{2}{s-M_N^2}\left(\frac{F_t(t)-1}{t-\mu_K^2} + H_t(s,t)\right)\\ &= eg\frac{2}{t-\mu_K^2}\left(\frac{F_s(s)-1}{s-M_N^2} + H_s(s,t)\right).\end{aligned} \tag{18}$$

To find the total correction to the Born amplitude one thus needs the coefficients multiplying $q^\mu$ in $\mathcal{L}^\mu_{[3]}$ [see (15)] and in $\mathcal{L}^\mu_{[4]}$ [see Eq. (16)] [alternatively $\Delta A_2$ can be expressed through $F_s(s)$ and $H_s(s,t)$]. It should be noted that $\Delta A_2$ cannot have poles, and the condition

$$\lim_{s\to M_N^2} H_t(s,t) = \frac{1-F_t(t)}{t-\mu_K^2} \tag{19}$$

should hold at $s=M_N^2$, which is the unphysical point for the $s$ channel.

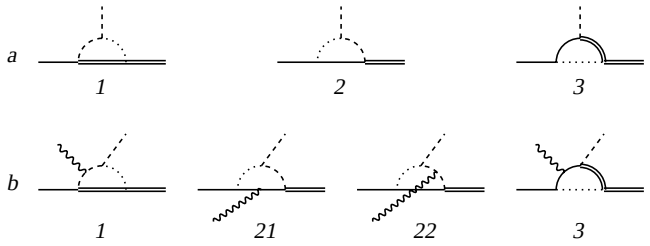


FIG. 2. One-loop corrections in the present model: $K^+p\Lambda$ vertex (a), four-point contribution $\mathcal{L}^\mu_{[4]}$ (b). Dotted lines correspond to the $\sigma$ meson, other notations are the same as in Fig. 1.

To calculate loop corrections we use an effective-Lagrangian model which is $SU(3)_{flavor}$ symmetrical and includes as degrees of freedom the baryon octet matrix $B$, the scalar ($J^P=1^+$) meson nonet $\Phi_s$, and the pseudoscalar ($J^P=1^-$) meson nonet $\Phi_{ps}$. The corresponding Lagrangian is

$$\begin{aligned}L = L_0 &+ D_s\mathrm{tr}(\Phi_s\{B,\bar{B}\}) + F_s\mathrm{tr}(\Phi_s[B,\bar{B}])\\ &+ D_{ps}\mathrm{tr}(\Phi_{ps}\{B,\bar{B}\}) + F_{ps}\mathrm{tr}(\Phi_{ps}[B,\bar{B}]) + L_\Phi,\end{aligned} \tag{20}$$

where $L_0$ is the free part, $\bar{B}=B^\dagger\gamma_0$, $[B,\bar{B}](\{B,\bar{B}\})$ stands for commutator (anticommutator), $D_s$ and $F_s$ ($D_{ps}$ and $F_{ps}$) are the baryon-meson coupling constants for scalars (pseudoscalars) [18], and $L_\Phi$ is the Lagrangian describing meson-meson interaction. The latter is chosen in the U(3) $\times$ U(3) linear $\sigma$ model [19] (the explicit form of $L_\Phi$ can be found, e.g., in Ref. [20]). For the purpose of our paper it is essential that $L_\Phi$ describes the $\sigma K^+K^-$ and $f_0K^+K^-$ couplings, where $\sigma\equiv f_0(400-1200)$ and $f_0\equiv f_0(980)$ [or $f_0(1370)$] represent the scalar mesons [21].

In the calculation of loops we do not include the $\pi$ meson and the $\Sigma$ hyperon in the intermediate states. This restricts the one-loop diagrams to those shown in Fig. 2. Calculation of the corresponding integrals is tedious and we refer to the Appendix for details.

The coupling constants of the SU(3) singlet $\phi_0$ and octet $\phi_8$ states to proton and $\Lambda$ follow from Eq. (20). To get couplings of the physical mesons, $\sigma$ and $f_0$, one needs in addition the mixing angle for the scalar mesons. All parameters are given in the Nijmegen baryon-baryon one-boson-exchange model of Ref. [18],

$$\begin{aligned}&g_{\sigma pp} = 16.90,\ g_{\sigma\Lambda\Lambda} = 9.84,\\ &g_{K^+p\Lambda} = -14.113,\ g_{f_0pp} = -2.97,\\ &g_{f_0\Lambda\Lambda} = -9.10,\end{aligned} \tag{21}$$

and masses $m_\sigma=0.76$ GeV, $m_{f_0}=0.993$ GeV. The corresponding vertex is $-ig_{\sigma BB}(-ig_{f_0BB})$. The $\sigma K^+K^-$ vertex is $-ig_{\sigma K^+K^-}$, with the coupling constant [20] $g_{\sigma K^+K^-}=\sqrt{3}(m_\sigma^2-\mu_K^2)/(2f_K)\sin(\alpha-\Delta\alpha)$, where $f_K=113$ MeV is the kaon weak-decay constant, $\alpha=\arcsin(1/\sqrt{3})\approx 35.26°$ is the "ideal" mixing angle, and $\Delta\alpha$ is a correction, usually of the order of $3°-10°$. Likewise, the $f_0K^+K^-$ vertex is $-ig_{f_0K^+K^-}$ with $g_{f_0K^+K^-}=\sqrt{3}(m_{f_0}^2-\mu_K^2)/(2f_K)\cos(\alpha-\Delta\alpha)$.

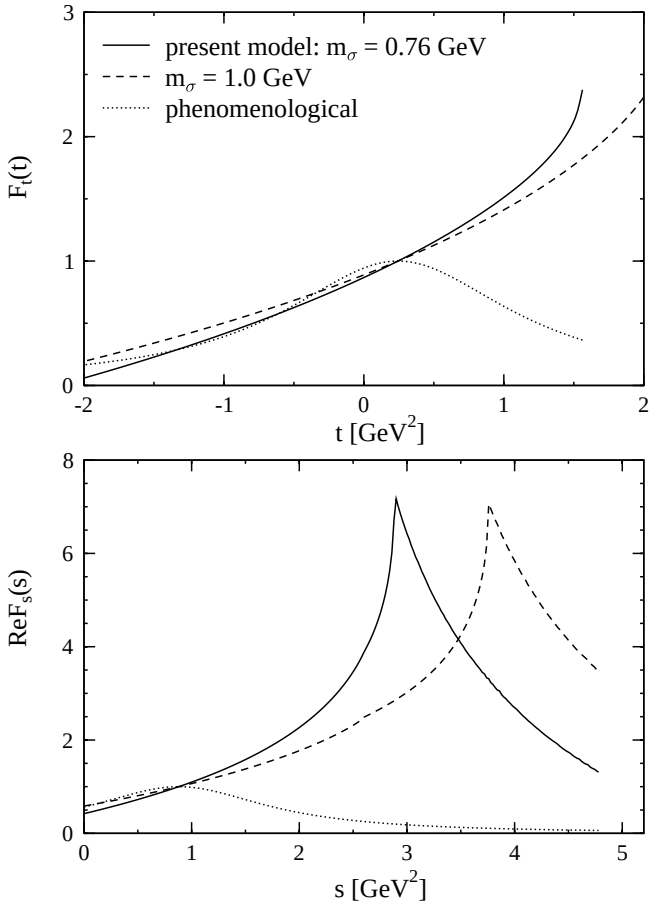


FIG. 3. Form factors in the $t$ channel (upper panel) and $s$ channel (lower panel). Solid and dashed lines present model with $m_\sigma$ =0.76 GeV and 1.0 GeV, respectively; dotted lines present phenomenological form factors from Eqs. (22).

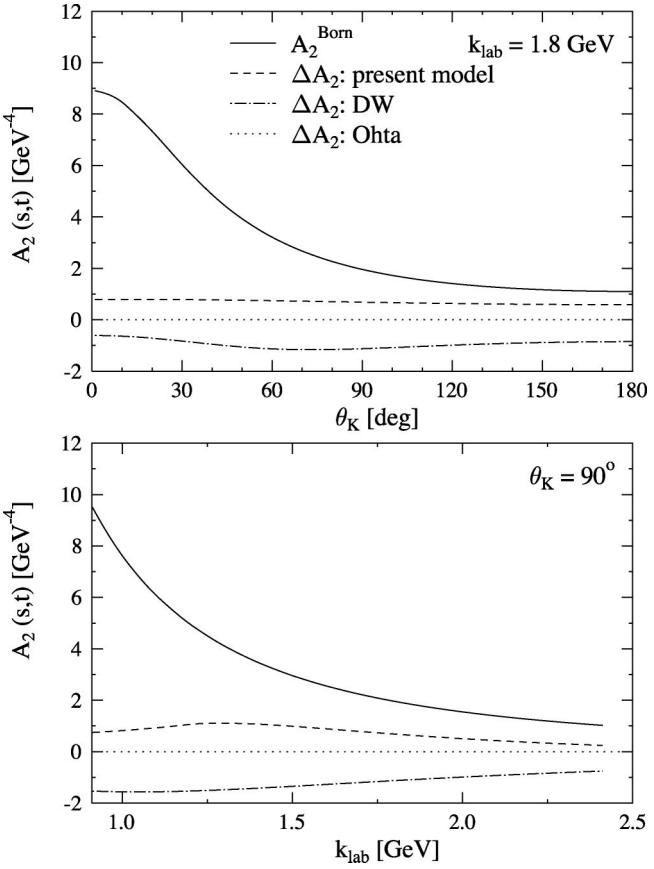


FIG. 4. Invariant amplitude $A_2(s,t)$ (real part) as function of scattering angle at fixed photon lab energy (top), and as function of energy at fixed angle (bottom). The calculation is performed with $m_\sigma$=0.76 GeV.

## III. RESULTS OF CALCULATION AND DISCUSSION

### A. Form factors and amplitude $A_2(s,t)$

In Fig. 3 we show the FF's as extracted from the loop corrections in the $t$ and $s$ channels for two masses of the $\sigma$ meson, 0.76 GeV and 1.0 GeV. For comparison the phenomenological FF's used in most analyses are also plotted. These have the typical bell-shape form (see, for example, Ref. [8])

$$F_s^{(ph)}(s) = \frac{\Lambda^4}{(s - M_N^2)^2 + \Lambda^4},$$

$$F_t^{(ph)}(t) = \frac{\Lambda^4}{(t - \mu_K^2)^2 + \Lambda^4} \qquad (22)$$

with a cutoff mass $\Lambda$ of about 1 GeV. All FF's are normalized to unity at the corresponding on-shell points. We do not present FF in the $u$ channel as it is not relevant for the discussion of the electric amplitude.

As it is seen from Fig. 3, $F_t(t)$ for $m_\sigma$=0.76 GeV is, in the physical region of the reaction $\gamma p \to K^+\Lambda$, rather close to the phenomenological FF down to $-1.5$ GeV$^2$. At positive $t$ the FF calculated in the present model keeps increasing and at $t=(\mu_K+m_\sigma)^2$ develops a cusp (not shown explicitly). The latter corresponds to the physical state of a kaon and a $\sigma$ in the $t$ channel ($p\bar{\Lambda} \to K^+$). The differences between $F_t(t)$ and $F_t^{(ph)}(t)$ at $t>0$ may not be considered very important, because this kinematical region is never reached in the $\gamma p \to K^+\Lambda$ reaction.

The $s$-channel FF is plotted in Fig. 3 up to $s \approx 5$ GeV$^2$ corresponding to photon lab energies $k_{lab}$ of about 2 GeV. Also here there is a sharp cusp at $s=(M_N+m_\sigma)^2$ that comes from the intermediate proton-$\sigma$ state depicted in diagrams 2 and 3 in Fig. 2(a). However, contrary to the $t$ channel, the difference between $F_s(s)$ and the phenomenological FF $F_s^{(ph)} \times(s)$ shows up in the physical region at $s \geqslant (M_\Lambda+\mu_K)^2$. For example, at $s$=3 GeV$^2$, corresponding to $k_{lab} \approx 1.1$ GeV, the FF $F_s(s)$ is larger than $F_s^{(ph)}(s)$ by a factor 30. This calculation shows that in microscopic models the FF's have much richer structure than the commonly used phenomenological parametrizations.

Figure 4 shows the correction to the Born amplitude calculated in the present model, and in the DW approach, Eq. (14), with FF's from Eq. (22). Ohta's recipe gives $\Delta A_2$=0. It is seen that loop corrections increase the Born amplitude $A_2^{Born}$, in contrast with the DW prediction. This result depends on the $\sigma$ mass; the calculation is performed with $m_\sigma$ =0.76 GeV and for the larger mass, $m_\sigma$=1 GeV, the correction is less.

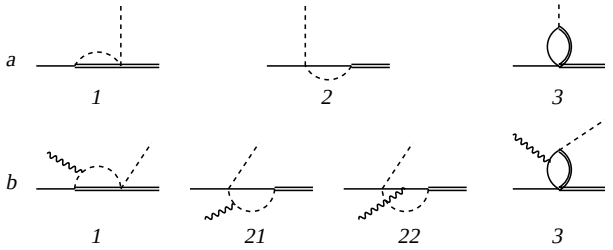


FIG. 5. Diagrams describing loop corrections to the three-point vertex (a) and four-point vertex (b), in which the $\sigma$ propagator has been contracted to a point. Notations are the same as in Figs. 1 and 2.

### B. Cancellation of loop corrections at large $m_\sigma$

With increasing $\sigma$-meson mass an interesting effect occurs: the total correction $\Delta A_2$ tends to zero in the loop calculation, implying a cancellation between the vertex corrections $\mathcal{L}^\mu_{[3]}$ and the four-point loop diagrams $\mathcal{L}^\mu_{[4]}$. This cancellation becomes more complete if $m_\sigma \gg M_N$ and $A_2 \to A_2^{Born}$. In other words, Ohta's prescription discussed in Sec. II B is reproduced.

There are two ways to understand this effect. One is by realizing that in general loop corrections to a strong vertex depend on the four-momenta of all particles involved. Minimal substitution in such a complicated function introduces many ambiguities as, for example, was discussed in Ref. [22]. In general, gauge-invariant tensor structures beyond the minimal substitution can be constructed through a combination of at least two four-vectors. For these four-vectors one may take the momenta of any particle involved and/or $\gamma$ matrices when dealing with fermions. The resulting terms may contribute to any of the tensors $\mathcal{M}^\mu_i$ with $i=1,2,3,4$. Therefore the minimal substitution in the most general $K^+p\Lambda$ vertex does not lead to unique results, even for $A_2(s,t)$.

If the vertex, however, depends on a single momentum $p^\mu$, then the procedure of minimal substitution gives unambiguous result for the electric amplitude. Possible terms beyond minimal substitution in such a vertex are expressed via $p^\mu$ and $\gamma^\mu$ solely. Any gauge-invariant structures built on these two four-vectors will not contribute to $\mathcal{M}^\mu_2$, which the present discussion is focused on, because the latter tensor involves two independent momenta $p^\mu$ and $p'^\mu$ [see Eq. (3)]. In this case any procedure to restore GI should thus yield identical results for the $A_2(s,t)$ amplitude.

The diagrams drawn in Fig. 5, which correspond to those of Fig. 2 in the limit $m_\sigma \to \infty$, help to understand the situation. In this limit the propagator of the $\sigma$ meson becomes momentum-independent and "shrinks" to a pointlike interaction, resulting in effective four-point vertices $\Lambda\Lambda K^+K^-, ppK^+K^-$, and $pp\Lambda\Lambda$. Simple analysis shows that, for example, diagram 1 in Fig. 5(a) depends exclusively on the nucleon momentum $p$ and does not depend on the kaon ($q$) and $\Lambda(p')$ momenta. Therefore this diagram can generate FF's depending on $s$ only, and cannot lead to any $u$ or $t$ dependencies. Similar arguments apply to other diagrams in Fig. 5(a). Any GI restoring procedure therefore gives result that coincides with that of Ohta [9], leading to complete cancellation between the vertex corrections and the contact terms. Of course this conclusion is valid only for the convection current related to $A_2$ and different procedures may give different results for the magnetic contributions associated with $A_1$, $A_3$, and $A_4$.

Another way to see the cancellation between the two contributions is to phrase the problem in terms of self-energy corrections. In the limit $m_\sigma \to \infty$ the vertex correction $\tilde{\Gamma}_1$ depends on $s=p^2$ and $\not{p}$ only and can be rewritten in terms of an irreducible vertex (which is pointlike in this limit) and a self-energy correction, $\tilde{\Gamma}_1 = (g/2f_K)\sqrt{3}\sin(\alpha-\Delta\alpha)\gamma_5\Sigma_N(p) \approx (g/2f_K)\gamma_5\Sigma_N(p)$. Since the vertex is normalized at the on-shell point $p^2=M_N^2$, the correction vanishes there, which implies that the self-energy also vanishes on shell, i.e., $\Sigma_N(p)u(p)=0$. The four-point term, shown in diagram 1 in Fig. 5(b), is proportional to $\tilde{\Gamma}^\mu(p+k,p)$, which corresponds to a photon coupling to the vertex correction $\tilde{\Gamma}_1$. It can be shown algebraically that

$$k_\mu \tilde{\Gamma}^\mu(p+k,p)u(p) = [\Sigma_N(p) - \Sigma_N(p+k)]u(p) = -\Sigma_N(p+k)u(p). \tag{23}$$

One may also argue that since the photon is coupled to all charged particles in the loop the vertex should obey the Ward-Takahashi identity [23] which reduces to Eq. (23) for the vertex correction.

The total correction to the Born amplitude can be written as

$$\frac{eg}{2f_K}\bar{u}(p')\gamma_5[\Sigma_N(p+k)S_0(p+k)\gamma^\mu + \tilde{\Gamma}^\mu(p+k,p)]u(p) \equiv \frac{eg}{2f_K}\bar{u}(p')\gamma_5 J^\mu u(p), \tag{24}$$

where $S_0(p+k)=(\not{p}+\not{k}-M_N)^{-1}$ is the free proton propagator. It is now straightforward to show that the current $J^\mu u(p)$ is (a) purely transverse, $k_\mu J^\mu u(p)=0$, and (b) independent of the momenta $p'$ of the $\Lambda$ and $q$ of the kaon. The first condition implies that the matrix element in Eq. (24) can be expressed in terms of the four Lorentz spin tensors $\mathcal{M}^\mu_i$, and the second implies that only $i=1,3$ are allowed. The contribution to the convection current therefore vanishes, i.e., $\Delta A_2=0$.

This result is general, although the arguments for the different diagrams in Fig. 5 differ in detail. Diagram 2 in Fig. 5(a), for example, describes the vertex correction $\tilde{\Gamma}_2$. This correction is proportional to an effective self-energy $\Sigma_\Lambda$ of the $\Lambda$. Since the final $\Lambda$ is on its mass shell this self-energy vanishes. The corresponding amplitude, proportional to $\tilde{\Gamma}_2$, vanishes as well. The four-point terms are given by the diagrams 21 and 22 in Fig. 5(b). Each of them is not zero, however they have opposite signs and cancel each other in $A_2$ when $m_\sigma \to \infty$. More formally, this result follows from the fact that diagrams 21 and 22 describe a correction $\tilde{\Gamma}^\mu(p',p'-k)$ to the EM vertex of the neutral $\Lambda$ hyperon, which is transverse, $k_\mu \cdot \tilde{\Gamma}^\mu(p',p'-k)=0$, and independent of the mo-

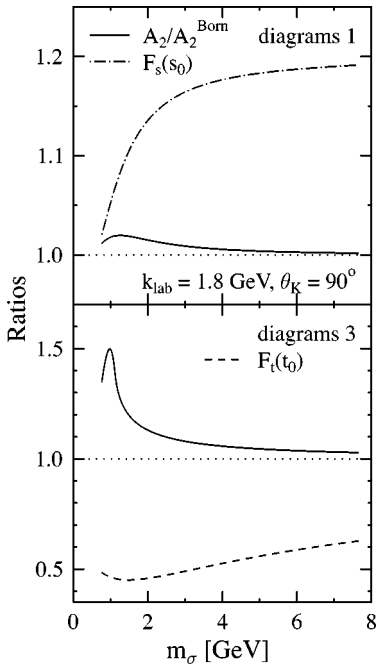


FIG. 6. Ratio $A_2/A_2^{Born}$ and form factors in the $s$ and $t$ channels as functions of $\sigma$-meson mass. Upper panel, calculation including only diagrams 1 in Fig. 2; lower panel, calculation including only diagrams 3 in Fig. 2. For diagrams 3 the coupling $g_{\sigma pp}g_{\sigma\Lambda\Lambda}$ is multiplied by $m_\sigma/0.76$ GeV. The invariant energy and momentum transfer corresponding to this kinematics are $s_0$=4.26 GeV$^2$ and $t_0$ =−1.05 GeV$^2$, respectively.

menta $p$ of the proton and $q$ of the kaon. Therefore these diagrams contribute to the tensors $\mathcal{M}_i^\mu$ with $i$=1,4 only, and $\Delta A_2$=0.

The situation with the corrections described by diagrams 3 in Fig. 5 is basically similar to diagrams 1. We only have to take into account that, since the couplings $g_{\sigma pp}$ and $g_{\sigma\Lambda\Lambda}$ are independent of $m_\sigma$, both three- and four-point corrections diminish if $m_\sigma\to\infty$. In order to observe effect of the cancellation, the diagrams have to be kept finite. One can assume, somewhat artificially, that the product $g_{\sigma pp}g_{\sigma\Lambda\Lambda}$ rises linearly with $m_\sigma$. A reasoning similar to that given above leads to the conclusion that $\Delta A_2$=0. Moreover, because the kaon is a spinless particle, the loop corrections do not contribute to the amplitudes $A_1$,$A_3$, and $A_4$ as well.

The above considerations are supported by numerical calculations (see Fig. 6). It is seen from the upper part of Fig. 6 that, when only the diagrams 1 in Fig. 2 are included, the FF $F_s(s)$ differs considerably from unity. This means that the correction to the three-point vertex does not vanish in the limit $m_\sigma\to\infty$ and yields the $s$ dependence of the vertex. In this limit the diagram should not contribute to the $t$-channel FF and indeed one finds that $F_t(t)\approx 1$ (not shown). At the same time the amplitude $A_2$ approaches the Born term at large $\sigma$ mass indicating the cancellation of all corrections as discussed above. It appears also that the corrections are small even at moderate $m_\sigma$. This is just a consequence of the fact that the coupling constants which enter this diagram are small.

If only the diagrams 3 in Fig. 2 are switched on, the $t$ dependence of the $K^+p\Lambda$ vertex is generated at all values of $m_\sigma$ (see the lower part of Fig. 6). Nonetheless the correction to the Born amplitude decreases fast and is practically negligible at $m_\sigma$ about 3–4 GeV. It is also interesting to note that at $m_\sigma\approx 1$ GeV the total correction is maximal. This reflects nonregular behavior of the four-point loop diagram as a function of invariant energy (cusp structure due to nucleon-$\sigma$ intermediate state).

The arguments presented above also justify our neglect of the proper self-energy insertions and corrections to the electromagnetic vertices, mentioned in the beginning of Sec. II C, in the calculation of the electric amplitude $A_2$.

We can conclude that in a microscopic model, where the three-point vertex has a particular structure which generates off-shell dependence only on a single momentum (corresponding to the limit where one of the particles in the loops is very heavy), different corrections to the Born amplitude cancel and the procedure of Ohta [9] is justified.

In more realistic models, in which light mesons are present in the loops, the corrections do not cancel and the DW procedure may be more appropriate. To test this assumption we calculated $\Delta A_2^{DW}$ in Eq. (14) with the microscopic FF's shown in Fig. 3, instead of phenomenological FF's used in the original formulation (one may argue however that only the phenomenological FF's are to be used in the DW approach). It turns out that at small $m_\sigma$ the correction $\Delta A_2^{DW}$ is of the same sign and similar magnitude as $\Delta A_2^{loops}$, however results disagree in the conditions where one is close to a threshold for the production of the physical particles included in the loop diagrams. While $\Delta A_2^{loops}$ is a flat and smooth background (see, for example, the dashed curve in Fig. 4, the DW calculation shows an irregular behavior reflecting the cusps in $F_s(s)$.

The above observations may support the picture in which the DW approach is applicable in the regime where loop corrections arise due to the light intermediate particles, while the method of Ohta is applicable in the other extreme.

The precise magnitude of the loop corrections depends of course on the detailed structure of the model. In the present semirealistic calculation, where pions and $\Sigma$ hyperons are not taken into account, the corrections tend to enhance the Born amplitude. This situation may however be reversed if all possible intermediate states are included.

Finally we should mention that the diagrams similar to those in Fig. 2, where $f_0$ meson replaces the $\sigma$, have also been included in the calculation. The effect of these turns out to be very small and can be discarded.

## IV. CONCLUSIONS

In the present work we have explicitly calculated loop corrections to the strong $K^+p\Lambda$ vertex and the additional four-point amplitude in an effective-Lagrangian model for photoinduced $K^+\Lambda$ production off the proton. The main focus has been on the scalar amplitude $A_2(s,t)$, associated with the electric contribution in a gauge-invariant approach.

The calculation shows that there is a strong cancellation in the amplitude $A_2(s,t)$ between three-point loop correc-

tions, often parametrized via form factors in a phenomenological approach, and four-point loop corrections, often written as contact terms restoring gauge invariance. This cancellation becomes complete if one of the intermediate particles in the diagrams becomes infinitely heavy. This shows that the result of the minimal-substitution method of Ohta [9] can be understood in the microscopic picture as a particular limiting case.

In a more realistic case the cancellation is not complete. Only part of the loop corrections can be absorbed in an appropriately chosen form factors and contact terms, constructed using the minimal substitution. The remaining part can be accounted through four-point contact terms which are gauge invariant and free of the poles, as was done in the work of DW [8,10].

The calculation also indicates that the form factors, usually taken in phenomenological approaches, may not be realistic. In a microscopic model the form factors are necessarily complex, with cusp structures in the real part reflecting the possibility that the intermediate states become physical particles for certain kinematical conditions. Even though we have focused our attention in this calculation on the electric current, we expect that the conclusion about the complex structure of the form factors is more general and applies to any vertex, which accounts for loop corrections not explicitly included in the present model. Nontrivial structures of the form factors extracted from a microscopic calculation were also observed in Ref. [5]. However the cancellation of different contributions which was observed in the calculation of the $A_2$ term may, due to the current conservation, be a peculiarity of the electric amplitude.

In the present calculation only the scalar mesons, proton, kaon, and $\Lambda$ hyperon have been included in the loop diagrams. In particular contributions involving the $\Sigma$ baryon and the pion have not been considered. Qualitatively one expects these particles to give similar contribution (in absolute magnitude and structure, but sign may be different) to what has been calculated in this work. Clearly a more complete calculation, where all possible intermediate states are taken into account, is needed to adequately describe the nonresonant part of the $\gamma p \to K^+\Lambda$ amplitude. The knowledge of the latter is imperative to separate the resonances from the background contribution in strangeness photoproduction.


## ACKNOWLEDGMENTS

Part of this work was performed as part of the research program of the Stichting voor Fundamenteel Onderzoek der Materie (FOM) with financial support from the Nederlandse Organisatie voor Wetenschappelijk Onderzoek (NWO). One of the authors (A.Yu.K.) acknowledges a grant from the NWO. He would also like to thank the staff of the Kernfysisch Versneller Instituut for the kind hospitality. We thank Rob Timmermans for helpful discussions.


## APPENDIX: EVALUATION OF LOOP INTEGRALS FOR THE $pK^+\Lambda$ VERTEX AND $\gamma p \to K^+\Lambda$ AMPLITUDE

The one-loop vertex corrections corresponding to the diagrams in Fig. 2(a) can be written as

$$\tilde{\Gamma}_1 = g g_{\sigma\Lambda\Lambda} g_{\sigma K^+K^-} \frac{i}{(2\pi)^4} \times \int \frac{\gamma_5(2M_\Lambda + \not{L})d^4L}{[(p'-L)^2 - M_\Lambda^2][(L+q)^2 - \mu_K^2](L^2 - m_\sigma^2)},$$

$$\tilde{\Gamma}_2 = g g_{\sigma pp} g_{\sigma K^+K^-} \frac{i}{(2\pi)^4} \times \int \frac{\gamma_5(M_N + \not{p} - \not{L})d^4L(2\pi)^{-4}}{[(p-L)^2 - M_N^2][(L-q)^2 - \mu_K^2](L^2 - m_\sigma^2)},$$

$$\tilde{\Gamma}_3 = g g_{\sigma pp} g_{\sigma\Lambda\Lambda} \frac{i}{(2\pi)^4} \times \int \frac{\gamma_5(2M_\Lambda + \not{L})(M_N + \not{p} - \not{L})d^4L(2\pi)^{-4}}{[(p-L)^2 - M_N^2][(p'-L)^2 - M_\Lambda^2](L^2 - m_\sigma^2)}, \tag{A1}$$

where we explicitly used Dirac equation for the final $\Lambda$, however did not assume the initial proton and the kaon to be on their the mass shells, i.e., $p^2 = s \neq M_N^2$ and $q^2 = t \neq \mu_K^2$. Using the Feynman parametrization and integrating over the loop momentum $L$ we obtain

$$\tilde{\Gamma}_1 = 2gC_1\gamma_5 \int_0^1 dx \int_0^x dy \frac{M_\Lambda(2-x) - \not{p}(x-y)}{\Delta_1(x,y)},$$

$$\tilde{\Gamma}_2 = 2gC_2\gamma_5 \int_0^1 dx \int_0^x dy \frac{M_N - M_\Lambda(x-y) + \not{p}(1-x)}{\Delta_2(x,y)},$$

$$\tilde{\Gamma}_3 = 2gC_3\gamma_5 \int_0^1 dx \int_0^x dy \Bigg\{ 2N_\epsilon - 1 - 2\ln\Delta_3(x,y) + \{M_N M_\Lambda(2-x+y) + M_\Lambda^2(2-x)(x-y) + \mu_K^2 y(x-y) + sy(1-x) + \not{p}[M_\Lambda(2-x-y) + M_N y]\} \frac{1}{\Delta_3(x,y)} \Bigg\}, \tag{A2}$$

with $C_1 = g_{\sigma\Lambda\Lambda} g_{\sigma K^+K^-}/32\pi^2$, $C_2 = g_{\sigma pp} g_{\sigma K^+K^-}/32\pi^2$, $C_3 = g_{\sigma\Lambda\Lambda} g_{\sigma pp}/32\pi^2$, and

$$\Delta_1(x,y) = M_\Lambda^2 xy - sy(x-y) + [\mu_K^2 - t(1-x)](x-y) + m_\sigma^2(1-x) - i0,$$

$$\Delta_2(x,y) = y[M_N^2 - s(1-x)] - M_\Lambda^2 y(x-y) + [\mu_K^2 - t(1-x)](x-y) + m_\sigma^2(1-x) - i0,$$

$$\Delta_3(x,y) = y[M_N^2 - s(1-x)] + M_\Lambda^2 x(x-y) - ty(x-y) + m_\sigma^2(1-x) - i0. \tag{A3}$$

While $\tilde{\Gamma}_1$ and $\tilde{\Gamma}_2$ are convergent, $\tilde{\Gamma}_3$ has a divergent piece which in the dimensional-regularization method is expressed

via the constant $N_\epsilon = 2/\epsilon - \gamma_E + \ln 4\pi$, where $\epsilon \equiv 4 - D$ and $D$ is the space-time dimension. In order to normalize the vertex we add a counterterm of the form $\delta g\, \gamma_5$ to the loop corrections. The coefficient $\delta g$ can be fixed by requiring $g$ to be the physical coupling constant $g_{K^+p\Lambda}$. This condition automatically makes the vertex finite and properly normalized to $g\gamma_5$ for on-mass-shell particles. Subsequently the off-shell vertex is calculated from

$$\bar{u}(p')\Gamma(p', p; q) = \bar{u}(p')[g\gamma_5 + \bar{\Gamma}_1 + \tilde{\Gamma}_2 + \tilde{\Gamma}_3 - (\tilde{\Gamma}_1 + \tilde{\Gamma}_2 + \tilde{\Gamma}_3)_{p^2 = M_N^2, q^2 = \mu_K^2}]. \quad \text{(A4)}$$

All FF's defined in Eqs. (5) and (6) of Sec. II B can be obtained from Eq. (A4). In particular, the $s$- and $t$-channel FF's are normalized as follows:

$$F_s(M_N^2) = F_t(\mu_K^2) = 1. \quad \text{(A5)}$$

There is an essential difference between the $s$ and $t$ channels. In the physical region of the $\gamma p \to K^+\Lambda$ reaction, where $t < 0$, the function $F_t(t)$ is real. In this case the dominators in Eqs. (A2) do not vanish and the calculation of the twofold integrals is straightforward. In the $s$ channel however the FF has an imaginary part which develops at $s \geqslant (M_\Lambda + \mu_K)^2$ for the first diagram in Fig. 2(a) and at $s \geqslant (M_N + m_\sigma)^2$ for the second and third diagrams. Calculation of the corresponding integrals requires care and we apply the methods developed by 't Hooft and Veltman in Ref. [24]. In particular, one integration in Eqs. (A2) can be performed which ensures that the remaining integrals are numerically stable.

The four-point loop contributions are shown in Fig. 2(b). We introduce the notation $\mathcal{L}^\mu_{[4]} = \mathcal{L}^\mu_{[4],1} + \mathcal{L}^\mu_{[4],21} + \mathcal{L}^\mu_{[4],22} + \mathcal{L}^\mu_{[4],3}$ for the four diagrams in Fig. 2(b). For example, for $\mathcal{L}^\mu_{[4],1}$ we have

$$\mathcal{L}^\mu_{[4],1} = egg_{\sigma\Lambda\Lambda} g_{\sigma K^+K^-} \frac{i}{(2\pi)^4} \int \frac{\gamma_5(2M_\Lambda + \not{L})[2(L^\mu + q^\mu) - k^\mu] d^4L}{[(p' - L)^2 - M_\Lambda^2][(L + q)^2 - \mu_K^2][(L + k - q)^2 - \mu_K^2](L^2 - m_\sigma^2)}, \quad \text{(A6)}$$

and similarly for $\mathcal{L}^\mu_{[4],21}, \mathcal{L}^\mu_{[4],22}$, and $\mathcal{L}^\mu_{[4],3}$ (the baryon spinors are omitted for brevity). One can explicitly check that these amplitudes satisfy the relation

$$\begin{aligned} k \cdot (\mathcal{L}_{[4]1} + \mathcal{L}_{[4]21} + \mathcal{L}_{[4]22} + \mathcal{L}_{[4],3}) &= -k \cdot \mathcal{T}_{El} \\ &= -e\bar{u}(p')[\Gamma(p', p + k; q) - \Gamma(p', p; q - k)]u(p), \end{aligned} \quad \text{(A7)}$$

which guarantees GI of the total amplitude.

We perform integration over $L$, as well as over one of the Feynman parameters. In order to obtain contribution of these loops to the coefficient $H_t(s,t)$ in Eq. (14) one has to project the tensor structure $\bar{u}(p')\gamma_5 q^\mu u(p)$ out of the final result. Any of the four-point integrals is proportional to the tensors: $\gamma_5\gamma^\mu, \gamma_5\gamma^\mu \not{k}, \gamma_5 p^\mu \not{k}, \gamma_5 q^\mu \not{k}, \gamma_5 p^\mu$, and $\gamma_5 q^\mu$, and of course terms $\propto \gamma_5 k^\mu, \gamma_5 k^\mu \not{k}$ can be dropped. It suffices for our purposes to select only those proportional to $\gamma_5 q^\mu$. In this way we arrive at the integrals with the following generic structure:

$$H_t(s,t) = \text{const}_1 \int_0^1 dx \int_0^x y dy \frac{\{1, x, x^2, y, y^2, xy\}}{A(A + By)} + \text{const}_2 \int_0^1 dx \ln \frac{M_\Lambda^2(1-x) + M_N^2 x - tx(1-x)}{M_\Lambda^2(1-x) + M_N^2 x - \mu_K^2 x(1-x)}, \quad \text{(A8)}$$

with the polynomials

$$A = ax^2 + by^2 + cxy + dx + ey + f - i0,$$
$$B = hx + jy + k. \quad \text{(A9)}$$

The coefficients $a, b, c, d, e, f, h, j, k$ depend on a particular diagram and are expressed in terms of the masses of external and internal particles, and the Mandelstam variables $s, u$, and $t$. The second integral in Eq. (A8) appears only in $\mathcal{L}^\mu_{[4],3}$. One integration can further be done using the methods of Ref. [24]. The obtained coefficients $H_t(s,t)$ for the diagrams in Fig. 2(b) are calculated numerically. In the numerical calculation double precision and a large number of mesh points are used to get accurate results.

[1] T. Mart, C. Bennhold, and C. E. Hyde-Wright, Phys. Rev. C **51**, R1074 (1995); J. C. David, C. Fayard, G. H. Lamot, and B. Saghai, *ibid.* **53**, 2613 (1996); R. A. Williams, C.-R. Ji, and S. R. Cotanch, *ibid.* **46**, 1617 (1992).
[2] T. Feuster and U. Mosel, Phys. Rev. C **59**, 460 (1999).
[3] G. Penner and U. Mosel, Phys. Rev. C **66**, 055212 (2002).
[4] S. Janssen, J. Ryckebusch, D. Debruyne, and T. Van Cauteren, Phys. Rev. C **65**, 015201 (2002); **66**, 035202 (2002).
[5] S. Kondratyuk and O. Scholten, Phys. Rev. C **64**, 024005 (2001).

[6] R. L. Workman, H. W. L. Naus, and S. J. Pollock, Phys. Rev. C **45**, 2511 (1992).
[7] H. Haberzettl, C. Bennhold, T. Mart, and T. Feuster, Phys. Rev. C **58**, R40 (1998).
[8] R. M. Davidson and Ron Workman, Phys. Rev. C **63**, 025210 (2001).
[9] K. Ohta, Phys. Rev. C **40**, 1335 (1989).
[10] R. M. Davidson and Ron Workman, Phys. Rev. C **63**, 058201 (2001).
[11] H. Haberzettl, Phys. Rev. C **56**, 2041 (1997).
[12] J. W. Bos, S. Scherer, and J. H. Koch, Nucl. Phys. **A547**, 488 (1992).
[13] J. Ball, Phys. Rev. **124**, 2014 (1961).
[14] W. A. Bardeen and Wu-Ki Tung, Phys. Rev. **173**, 1423 (1968).
[15] M. Gell-Mann and M. L. Goldberger, Phys. Rev. **96**, 1433 (1954).
[16] E. Kazes, Nuovo Cimento **XIII**, 1226 (1959).
[17] O. Scholten, A. Yu. Korchin, V. Pascalutsa, and D. Van Neck, Phys. Lett. B **384**, 13 (1996); A. Yu. Korchin, O. Scholten, and R. G. E. Timmermans, *ibid.* **438**, 1 (1998).
[18] P. M.M. Maessen, Th. A. Rijken, and J. J. de Swart, Phys. Rev. C **40**, 2226 (1989).
[19] M. Lèvy, Nuovo Cimento A **52**, 23 (1967).
[20] N. A. Tornqvist, Eur. Phys. J. C **11**, 359 (1999).
[21] K. Hagiwara *et al.*, Particle Data Group, Phys. Rev. D **66**, 010001 (2002), URL: http://pdg.lbl.gov
[22] S. Kondratyuk and O. Scholten, Nucl. Phys. **A677**, 396 (2000).
[23] C. Itzykson and J.-B. Zuber, *Quantum Field Theory* (McGraw-Hill, New York, 1986), Chap. 7.1.
[24] G. 't Hooft and M. Veltman, Nucl. Phys. **B153**, 365 (1979).